Available online at www.sciencedirect.com
ScienceDirect
International Communications in Heat and Mass Transfer 34 (2007) 653 – 660
International Communications in HEAT and MASS TRANSFER
www.elsevier.com/locate/ichmt

Photographic study of high-flux subcooled flow boiling and critical heat flux☆

Hui Zhang [a], Issam Mudawar [a,*], Mohammad M. Hasan [b]

[a] *Boiling and Two-phase Flow Laboratory, School of Mechanical Engineering, Purdue University, West Lafayette, IN 47907, USA*
[b] *NASA Glenn Research Center, 21000 Brookpark Road, Cleveland, OH 44135, USA*

Available online 22 March 2007

Abstract

This study examines both high-flux flow boiling and critical heat flux (CHF) under highly subcooled conditions using FC-72 as working fluid. Experiments were performed in a horizontal flow channel that was heated along its bottom wall. High-speed video imaging and photomicrographic techniques were used to capture interfacial features and reveal the sequence of events leading to CHF. At about 80% of CHF, bubbles coalesced into oblong vapor patches while sliding along the heated wall. These patches grew in size with increasing heat flux, eventually evolving into a fairly continuous vapor layer that permitted liquid contact with the wall only in the wave troughs between vapor patches. CHF was triggered when this liquid contact was finally halted. These findings prove that the CHF mechanism for subcooled flow boiling is consistent with the interfacial lift-off mechanism proposed previously for saturated flow boiling.

Keywords: Critical heat flux; Flow boiling; Subcooled boiling

1. Introduction

Subcooled flow boiling is wildly used in applications demanding the removal of high heat fluxes while maintaining relatively low surface temperatures. They include nuclear reactor cores, lasers, advanced microprocessors, and hybrid vehicle power electronics. A primary goal in all these applications is to maintain subcooled flow boiling while making certain the operating heat flux is safely below the critical heat flux (CHF). CHF for these and many other heat flux controlled applications is the result of a sudden, sharp decrease in the convective heat transfer coefficient, as liquid access to the surface that is essential to maintaining the boiling process is interrupted. CHF amounts to catastrophic failure because of the ensuing runaway increase in surface temperature. This is why predicting CHF remains one of the most important fundamental problems in the heat transfer literature.

Coupled with the urgency to establish safety guidelines for flux-controlled flow boiling applications, the complexity of the CHF mechanism has steered the vast majority of CHF studies in the direction of empirical formulation. A

☆ Communicated by W.J. Minkowycz.
* Corresponding author.
E-mail address: mudawar@ecn.purdue.edu (I. Mudawar).

0735-1933/$ - see front matter © 2007 Elsevier Ltd. All rights reserved.
doi:10.1016/j.icheatmasstransfer.2007.01.014

Nomenclature

CHF	critical heat flux
g_e	gravitational acceleration
T	temperature
$\Delta T_{sub,o}$	subcooling at downstream edge of heated section of channel, $T_{sat,o} - T_o$
U	mean liquid velocity at inlet to heated section of channel

Subscripts

o	outlet of heated section of channel
sat	saturation

continuing concern with the use of CHF correlations has been the limited range of operating conditions for the experiments these correlations are based upon, let alone the effects of secondary parameters (e.g., pump type, surface roughness, etc.) sometimes ignored when constructing a new correlation. These limitations bring into question a popular tendency to extrapolate existing CHF correlations to fluids and/or operating conditions beyond those for which the correlations are recommended.

A more convincing approach to predicting flow boiling CHF is to develop mechanistic models based on photographic analysis of the vapor layer development along a heated wall at conditions leading to, and including the CHF point. Such models could ultimately replace empirical correlations and extend prediction domain to different fluids, flow geometries and broad ranges of operating conditions.

Mechanistic flow boiling CHF models fall into four main types: *boundary layer separation*, *bubble crowding*, *sublayer dryout*, and *interfacial lift-off*. Boundary layer separation models postulate that the liquid velocity gradient is decreased at CHF to the point of liquid stagnation by the vapor production at the wall [1,2]. Eventually, the bulk liquid flow separates from the heated wall, and dryout ensues. The bubble crowding mechanism is based on the assumption that CHF occurs when turbulent fluctuations in the liquid flow become too weak to transport liquid through the dense bubbly wall layer in order to cool the wall [3,4]. The sublayer dryout model is based on the premise that CHF will occur when the wall heat flux surpasses the enthalpy of liquid replenishing a wall liquid sublayer from the bulk liquid [5–7]. The interfacial lift-off model is the most recent of these models. It describes the sequence of events preceding CHF occurrence as well as the trigger event for CHF. The vapor layer is described as a series of vapor patches that propagate along the heated wall, and the trigger event as the separation of wetting fronts between the vapor patches [8–13]. The interfacial lift-off mechanism has enabled theoretical formulation of CHF models for a variety of pool boiling and flow boiling configurations [14]. Unfortunately, this model has been formulated only for near-saturated flow boiling conditions. The present study concerns highly subcooled flow boiling.

In the present study, advanced high-speed video imaging and photomicrographic techniques were utilized to capture the vapor layer evolution with increasing heat flux at conditions leading to, and including the CHF point.

2. Experimental methods

The experimental techniques adopted in the present study are identical to those described by the authors in a prior study [14], therefore only a brief description is provided here. A mostly transparent flow boiling test module was fabricated that enabled side viewing of vapor layer evolution along a heated wall. As shown in Fig. 1(a), the boiling module featured a 5.0×2.5 mm^2 flow channel that was fitted along one side with a heated wall. As shown in Fig. 1(b), the heated wall consisted of a 0.56 mm-thick oxygen-free copper plate that was heated by a series of thick-film electrical resistors. The flow was allowed to develop upstream of the heated wall over an entrance length 106 times the channel's hydraulic diameter to ensure fully-developed flow. Fluid temperature and pressure were measured just upstream and downstream of the heated wall.

FC-72 liquid was supplied to the flow boiling module at controlled pressure, temperature and flow rate using the flow loop depicted schematically in Fig. 1(c). Using this flow loop, CHF values were measured for the following operating conditions: outlet pressure of 138–152 kPa (20–22 psia), outlet subcooling of $\Delta T_{sub,o} = 10$–30 °C (photographic studies were also performed at 40 °C),

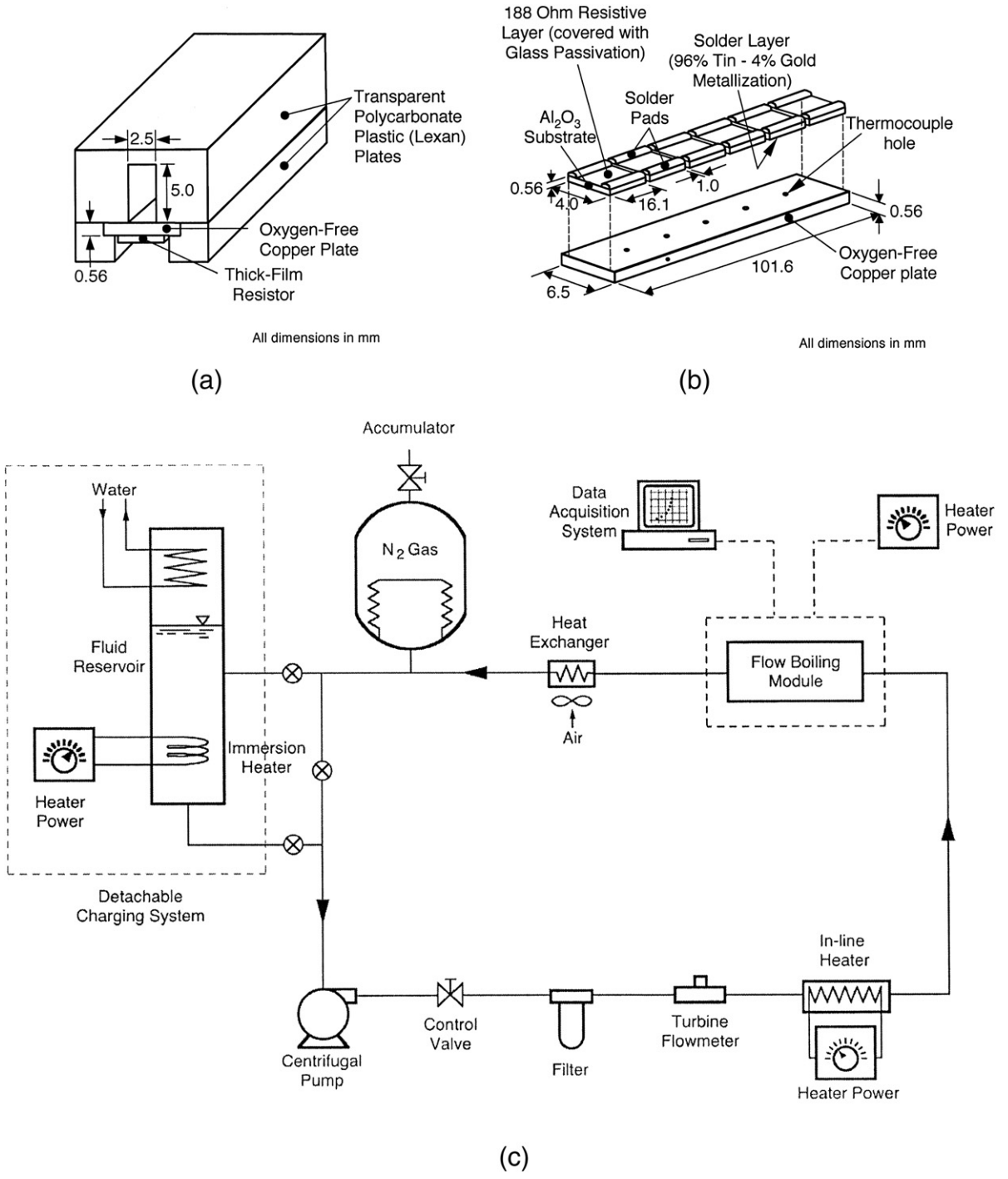

Fig. 1. (a) Flow channel assembly. (b) Construction of heated wall. (c) Two-phase flow loop.

and inlet liquid velocity of $U=0.5–1.5$ m/s. Uncertainties in the flow rate, heat flux and temperature measurements were 2.3%, 0.2%, and 0.3 °C, respectively.

A FASTCAM-Ultima APX FM high-speed digital video system was used to capture the evolution of the vapor layer along the heated wall. This system is capable of recording 2000 frames/s at full resolution of 1024×1024, and up to 120,000 frames/s at

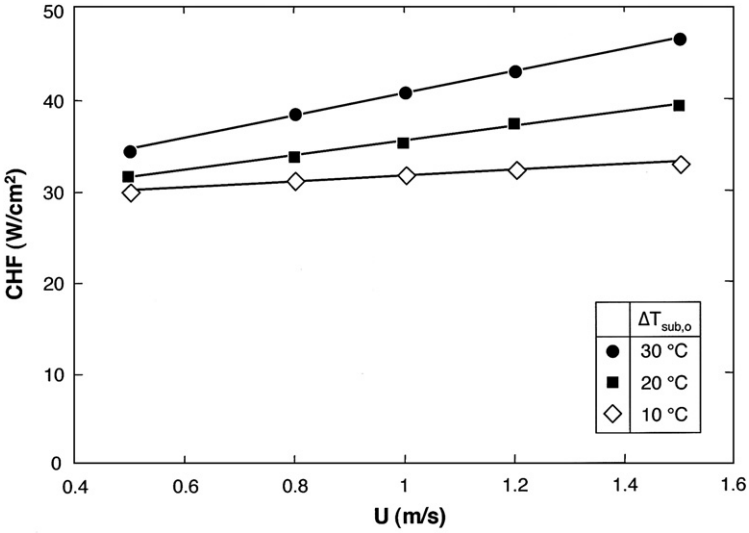

Fig. 2. Variation of CHF with mean inlet liquid velocity for three subcoolings.

reduced resolution. The shutter speed of this system could be varied from 1/60th s to 4 μs depending on frame rate. To magnify small interfacial features, the video camera was fitted with an Infinity K-3 lens, which yielded up to 10 times magnification. Most of the video images presented in the this paper were captured with 1024×1024 resolution at 2000 frames/s and a shutter speed of 80 μs.

3. Experimental results

Fig. 2 shows the variation of measured CHF with mean inlet velocity for three subcoolings. CHF increased monotonically with increasing velocity, and increasing subcooling increased both CHF and the sensitivity of CHF to flow velocity. This trend points to the important role of subcooling to the evolution of the vapor layer.

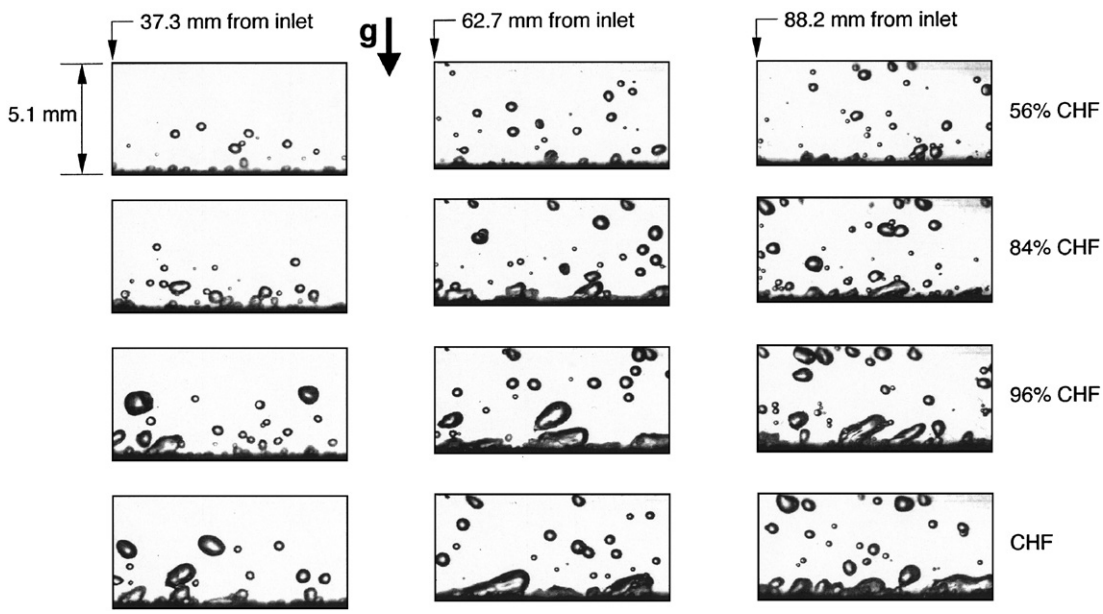

Fig. 3. Vapor layer development along heated wall for U=0.5 m/s and $\Delta T_{sub,o}$=40 °C corresponding to different heat fluxes leading to CHF.

Fig. 3 depicts the development of the vapor layer along the heated wall for a relatively low velocity of U=0.5 m/s and $\Delta T_{sub,o}$= 40 °C. Shown are representative images of the vapor layer whose leading edges are 37.2, 62.7 and 88.2 mm from the leading edge of the heated wall at four heat fluxes ranging from 56% to 100% of CHF. At 56% of CHF, Fig. 3 shows individual bubbles detach from

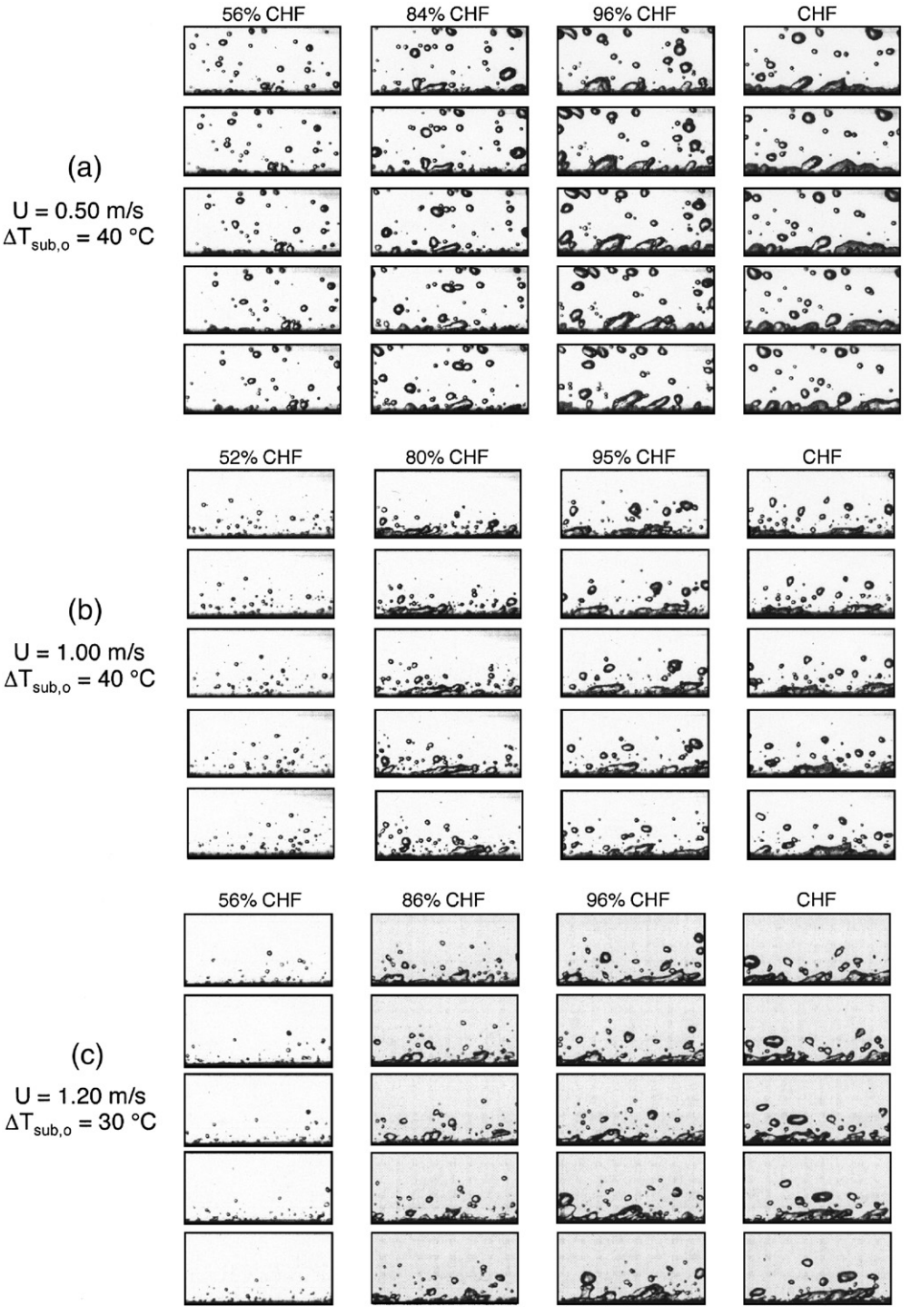

Fig. 4. Sequential images of vapor layer at different heat fluxes leading to CHF for (a) U=0.5 m/s and $\Delta T_{sub,o}$=40 °C, (b) U=1.0 m/s and $\Delta T_{sub,o}$= 40 °C, and (c) U=1.2 m/s and $\Delta T_{sub,o}$=30 °C.

the wall and are entrained in the bulk liquid flow as other bubbles slide along the wall. The entrained bubbles grow in number along the channel while some of the sliding wall bubbles coalesce into larger bubbles downstream. At 84% of CHF, a larger number of bubbles detach from the wall and increase in number downstream; these bubbles are generally bigger than at 56%. The sliding wall bubbles at 84% begin to coalesce into oblong bubbles that grow in both size and number along the heated wall. At 96% of CHF, entrained bubbles grow further in size, and the oblong bubbles sliding along the wall grow closer, producing a seemingly continuous wavy vapor layer spanning both the middle and downstream regions of the heated wall. Close inspection of this vapor layer shows liquid could still contact the heated wall in wetting fronts between the oblong vapor patches. At CHF, the vapor layer fully engulfs the heated wall, precluding liquid contact even in the wetting fronts.

Fig. 4 captures temporal variations of the vapor layer along the downstream section of the heated wall with increasing heat flux for three velocities at relatively high subcooling. Five sequential images are depicted for each velocity, heat flux and subcooling condition. Consecutive images are separated by 0.001 s. Several trends are common to all three velocities. Namely, some bubbles are entrained in the bulk liquid flow while most of the vapor is confined to the wall where it exhibits appreciable coalescence with increasing heat flux. Oblong vapor patches in each case coalesce into a fairly continuous wavy vapor layer slight before CHF. The vapor patches themselves constitute crests in the wavy layer, and are separated by toughs – wetting fronts – where liquid is able to make contact with the wall. The liquid replenishment is extinguished at CHF as the troughs themselves are fully engulfed in vapor. Comparing Fig. 4(a), (b) and (c) shows flow velocity has a noticeable effect on vapor distribution across the channel. Given the relatively weak drag force at $U=0.5$ m/s, detached bubbles are more easily separated from the wall by buoyancy and driven toward the top wall of the channel. At 1.0 m/s, Fig. 4(b), and 1.2 m/s, Fig. 4(c), the increased drag force prevents vapor bubbles from traveling across the channel, maintaining most of the vapor in close proximity to the heated wall. While not readily apparent form the images in Fig. 4, subcooling has a profound influence on all stages of the vapor layer development. In fact, the overall thickness of the vapor layer for all subcooled conditions captured in the present study is far thinner than for saturated flow boiling at the same velocity [14]. There is also a combined effect of velocity and subcooling that is evident in the increasing slope of CHF versus velocity with increasing subcooling as shown earlier in Fig. 2.

To better understand the formation of the wavy vapor layer by coalescence of adjacent vapor patches, high magnification lenses were used to capture the near-wall region of the channel. Fig. 5 shows the formation of a wave crest and dryout of wetting fronts both upstream and downstream of the crest as heat flux is increased toward CHF for $U=1.2$ m/s and $\Delta T_{sub,o}=30$ °C. The three consecutive images shown for each heat flux condition are separated by 0.0005 s.

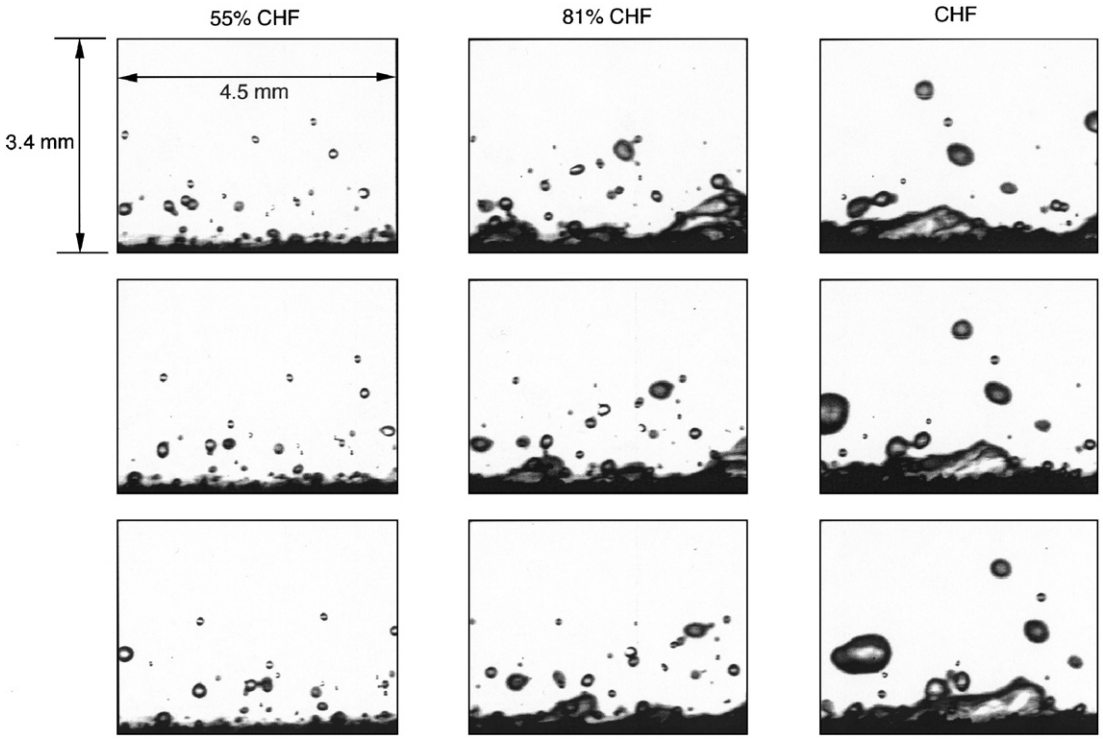

Fig. 5. Magnified sequential images of vapor layer at different heat fluxes leading to CHF for $U=1.2$ m/s and $\Delta T_{sub,o}=30$ °C.

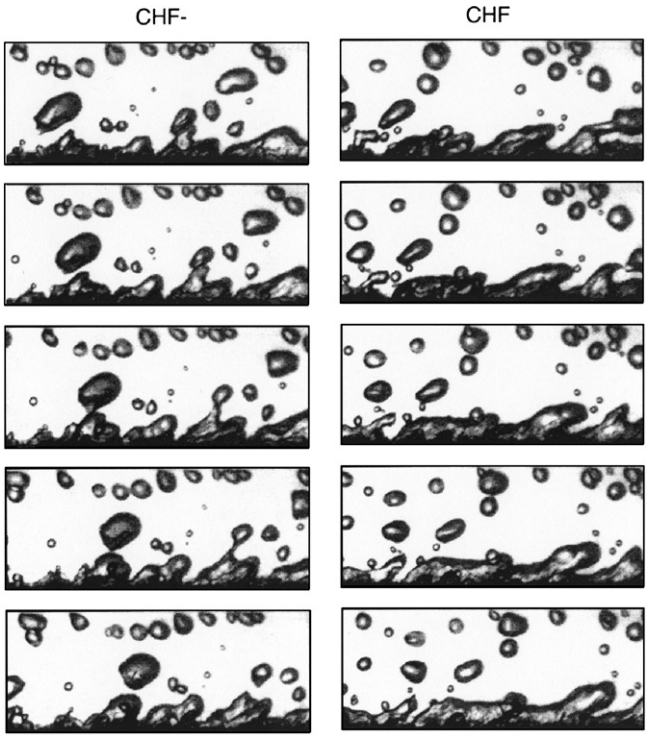

Fig. 6. Sequential images of CHF transient for $U=0.5$ m/s and $\Delta T_{sub,o}=30$ °C.

Fig. 6 provides further evidence of this CHF mechanism. Conditions were captured during the CHF transient at $U=0.5$ m/s and $\Delta T_{sub,o}=30$ °C. Notice the loss of liquid access to the wall between vapor patches as the vapor layer fully engulfs the heated wall.

4. Conclusions

This study explored the CHF mechanism in highly subcooled flow boiling. CHF increases monotonically with increases in flow velocity and/or subcooling. High-speed video imaging revealed a sequence of events that culminate in CHF. While some bubbles are detached from the wall and entrained in the bulk liquid flow, the majority of the vapor remains in close proximity to the wall, especially at high flow velocities. Bubbles first slide along the heated wall, coalescing with other bubbles to form oblong vapor patches. These patches propagate along the heated wall, growing in size and proximity with increasing heat flux. Just before CHF, the series of vapor patches evolve into a fairly continuous vapor layer that permits liquid contact with the heated wall only in the wave troughs – wetting fronts – between the vapor patches. At CHF, these wetting fronts are extinguished as the vapor layer prevents any further liquid contact. These findings prove that the CHF mechanism for subcooled flow boiling is identical to the interfacial lift-off mechanism proposed previously for saturated flow boiling.

Acknowledgement

The authors are grateful for the support of the National Aeronautics and Space Administration under Grant No. NNC04GA54G.

References

[1] S.S. Kutateladze, A.I. Leont'ev, Some applications of the asymptotic theory of the turbulent boundary layer, Proceedings of the 3rd International Heat Transfer Conference, Chicago, Illinois, 1966.

[2] L.S. Tong, Boundary layer analysis of the flow boiling crisis, Int. J. Heat Mass Transfer 11 (1968) 1208–1211.
[3] J. Weisman, B.S. Pei, Prediction of critical heat flux in flow boiling at low qualities, Int. J. Heat Mass Transfer 26 (1983) 1463–1477.
[4] J. Weisman, S. Ileslamlou, A phenomenological model for prediction of critical heat flux under highly subcooled conditions, Fus. Technol. 13 (1988) 654–659.
[5] C.H. Lee, I. Mudawar, A mechanistic critical heat flux model for subcooled flow boiling based on local bulk flow conditions, Int. J. Multiph. Flow 14 (1989) 711–728.
[6] Y. Katto, A physical approach to critical heat flux of subcooled flow boiling in round tubes, Int. J. Heat Mass Transfer 33 (1990) 611–620.
[7] G.P. Celata, M. Cumo, Y. Katto, A. Mariani, Prediction of the critical heat flux in water subcooled flow boiling using a new mechanistic approach, Int. J. Heat Mass Transfer 42 (1999) 1457–1466.
[8] J.E. Galloway, I. Mudawar, CHF mechanism in flow boiling from a short heated wall — part 1. Examination of near-wall conditions with the aid of photomicrography and high-speed video imaging, Int. J. Heat Mass Transfer 36 (1993) 2511–2526.
[9] J.E. Galloway, I. Mudawar, CHF mechanism in flow boiling from a short heated wall — part 2. Theoretical CHF model, Int. J. Heat Mass Transfer 36 (1993) 2527–2540.
[10] J.C. Sturgis, I. Mudawar, Critical heat flux in a long, rectangular channel subjected to one-sided heating — I. Flow visualization, Int. J. Heat Mass Transfer 42 (1999) 1835–1847.
[11] J.C. Sturgis, I. Mudawar, Critical heat flux in a long, rectangular channel subjected to one-sided heating — II. Analysis of critical heat flux data, Int. J. Heat Mass Transfer 42 (1999) 1849–1862.
[12] H. Zhang, I. Mudawar, M.M. Hasan, Experimental assessment of the effects of body force, surface tension force, and inertia on flow boiling CHF, Int. J. Heat Mass Transfer 45 (2002) 4079–4095.
[13] H. Zhang, I. Mudawar, M.M. Hasan, Experimental and theoretical study of orientation effects on flow boiling CHF, Int. J. Heat Mass Transfer 45 (2002) 4463–4478.
[14] H. Zhang, I. Mudawar, M.M. Hasan, Flow boiling CHF in microgravity, Int. J. Heat Mass Transfer 48 (2005) 3107–3118.